Electrical Impedance Tomographic Mapping of Hypoventilated Lung Areas in Intubated Patients With COVID-19

Débora S Caetano, Caio CA Morais, Wagner S Leite, Rômulo de Aquino C Lins, Kyle J Medeiros, Rodrigo A Cornejo, Armèle Dornelas de Andrade, Shirley L Campos, and Daniella C Brandão

Introduction

Since the first description of ARDS, bilateral alveolar infiltrates on chest radiography have been recognized as characteristic of this syndrome, combined with hypoxemia and low respiratory system compliance (C_{RS}).[1] Due to its simplicity, chest radiography is still a pillar of the actual ARDS definition.[2] However, only the advance to chest computed tomography (CT) allowed clinicians to precisely identify the site of lung disease, revealing the heterogeneous distribution of lung injury in patients with ARDS.[3,4] As with previous ARDS descriptions, CT studies reported a variety of areas with pulmonary involvement in subjects with COVID-19,[5,6] such as multilobar ground-glass opacities and consolidation located mainly in the gravity-dependent regions.

The use of a chest CT to phenotype ARDS as a focal or non-focal disease is also advocated to allow personalized mechanical ventilation.[7] However, the use of CT is limited by the ionizing radiation and the need for patient transfer.[8] In this scenario, electrical impedance tomography (EIT) has been used at the bedside to monitor pulmonary function in real time during mechanical ventilation.[9,10] In this report, we aimed to describe the distribution pattern of hypoventilated regions (ie, areas with deteriorated lung function) in patients with COVID-19–related ARDS under invasive mechanical ventilation with the use of EIT. In addition, we assessed the relationship between the distribution pattern of hypoventilated regions with C_{RS} and gas exchange (P_{aO_2}/F_{IO_2}).

Methods

This study is a secondary analysis of a clinical trial (https://clinicaltrials.gov, NCT 05024500) that consecutively monitored subjects with EIT who had been admitted to a tertiary ICU from October 2020 to June 2021. All the subjects were ventilated in the volume-controlled mode (tidal volume of 6 mL/kg of predicted body weight) for < 72 h, with PEEP of 10 cm H_2O as recommended previously by Villar et al.[11] In this analysis, we excluded subjects on assisted or spontaneous ventilation modes and with a P_{aO_2}/F_{IO_2} of 300 mm Hg on the day of assessment.

The EIT images were acquired by using Enlight-1800 (Timpel Medical, São Paulo, Brazil) with the electrode strap positioned around the patient's chest at the axillar level. The subjects were in the supine position, with the head tilted at 30°. The lung images were divided into 4 regions of interest (ROI): upper right (UR), lower right (LR), upper left (UL), and lower left (LL). The regional distribution of ventilation was determined as a percentage of the change in

Ms Caetano, Dr Morais, Mr Leite, Mr Lins, Dr de Andrade, Dr Campos, and Dr Brandão are affiliated with the Physiotherapy Department, Universiade Federal de Pernambuco, Recife, Brazil. Dr Morais is affiliated with the Laboratório de Pneumologia LIM-09, Disciplina de Pneumologia, Heart Institute (Incor), Hospital das Clínicas da Faculdade de Medicina da Universidade de São Paulo, Brazil. Dr Medeiros is affiliated with the Department of Anesthesia, Critical Care and Pain Medicine, Massachusetts General Hospital and Harvard Medical School, Boston, Massachusetts. Dr Cornejo is affiliated with the Unidad de Pacientes Críticos, Departamento de Medicina, Hospital Clínico Universidad de Chile, Santiago, Chile.

Ms Caetano and Dr Morais contributed equally to this work.

Correspondence: Daniella C Brandão PhD, Physiotherapy Department, Universidade Federal de Pernambuco, Av. Jorn. Aníbal Fernandes, 173, Recife, Pernambuco 50740-560, Brazil. E-mail: daniella.brandao@ufpe.br.
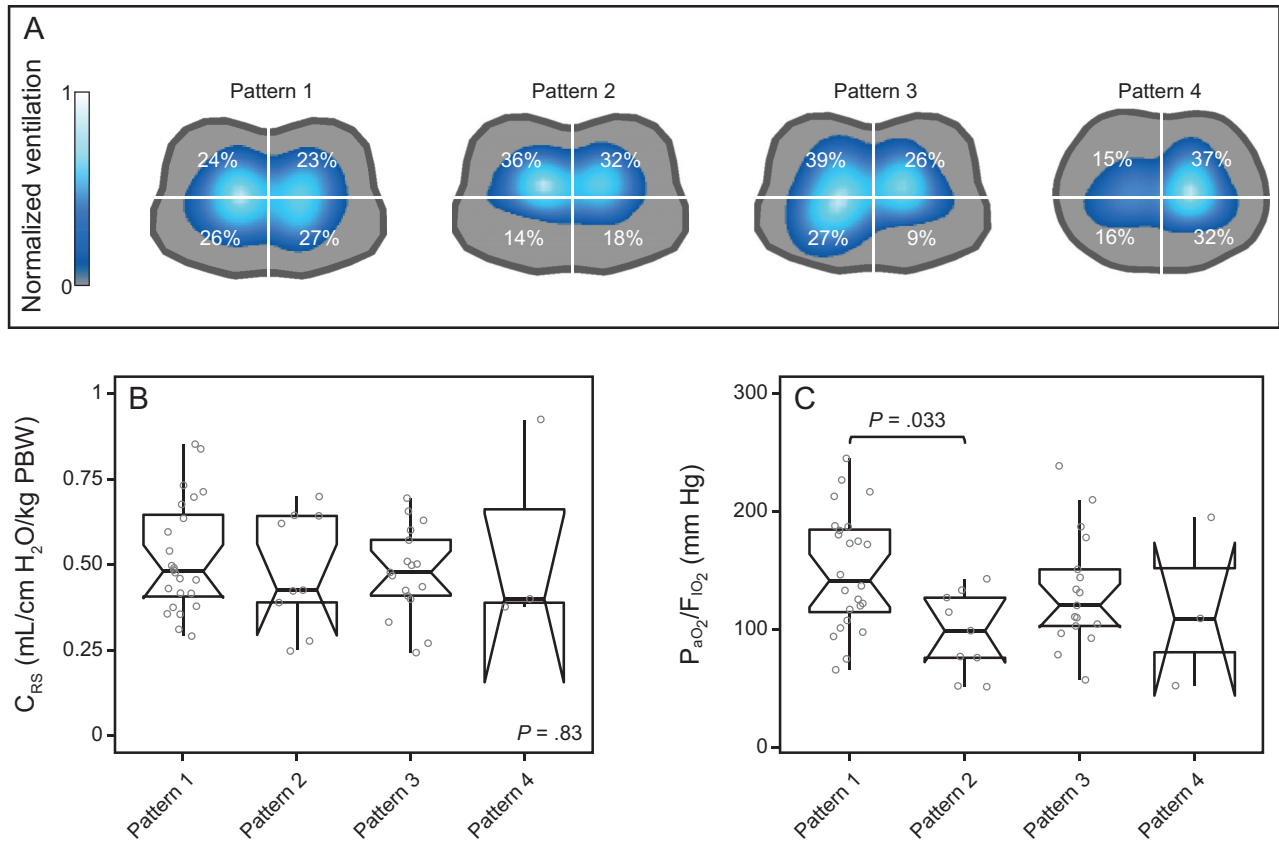
Fig. 1. A: Illustration of the distribution of hypoventilated regions patterns detected by electrical impedance tomography (EIT): pattern 1, preserved bilateral dorsal ventilation ($ZV_{LR} + ZV_{LL} > 40\%$); pattern 2, bilateral dorsal hypoventilation ($ZV_{LR} + ZV_{LL} < 40\%$); pattern 3, unilateral dorsal hypoventilation (ZV_{LR} or $ZV_{LL} < 20\%$); and pattern 4, unilateral hypoventilation ($ZV_{UR} + ZV_{LR}$ or $ZV_{UL} + ZV_{LL} < 40\%$). The color scale of the EIT image was normalized by the sum of the impedance values within the lung area (the lighter the blue, the greater the regional ventilation). B: Respiratory-system compliance (C_{RS}) normalized by predicted body weight. C: P_{aO_2}/F_{IO_2} according to the hypoventilation pattern. Box plots in panels B and C express median, 25% and 75% quartiles, minimum and maximum, and outliers (>1.5 interquartile length values).

impedance for each quadrant in relation to the total change in impedance:

$$ZV_{ROI} = \frac{\Delta Z_{ROI}}{\Delta Z_{total}} \times 100$$

The distribution of hypoventilated regions was stratified into 4 patterns (or phenotypes): pattern 1, preserved bilateral dorsal ventilation ($ZV_{LR} + ZV_{LL} > 40\%$); pattern 2, bilateral dorsal hypoventilation ($ZV_{LR} + ZV_{LL} < 40\%$); pattern 3, unilateral dorsal hypoventilation (ZV_{LR} or $ZV_{LL} < 20\%$); and pattern 4, unilateral hypoventilation ($ZV_{UR} + ZV_{LR}$ or $ZV_{UL} + ZV_{LL} < 40\%$) (Fig. 1A).

Respiratory system mechanics and arterial blood gases were assessed during EIT assessment. C_{RS} was calculated as expiratory tidal volume divided by the difference between plateau pressure and total PEEP. The plateau pressure and total PEEP were measured by using an end-inspiratory occlusion of 0.5 s and an end-expiratory occlusion of 2 s, respectively. C_{RS} was normalized by the predicted body weight to

account for differences in height and sex (eg, a normalized compliance of 0.5 mL/cm H_2O/kg predicted body weight would correspond to 35 mL/cm H_2O for a 70-kg patient).

Statistical Analysis

Continuous variables were expressed as median (interquartile range), and categorical variables were expressed as frequencies (percentages). Differences between groups were assessed with Kruskal-Wallis test, followed by the Dunn post hoc test. Differences were considered significant with $P < .05$. The analysis was conducted by using RStudio (v1.1.456; PBC, Boston, Massachusetts) and R Statistical Software (v3.6.2; R Foundation for Statistical Computing, Vienna, Austria).

Results

A total of 53 subjects were included in this analysis (Table 1): 24 subjects (45%) showed preserved bilateral

Table 1. Characteristics of the Subjects at Baseline

Characteristic	Pattern 1	Pattern 2	Pattern 3	Pattern 4
Subjects	24 (45.3)	9 (17)	17 (32)	3 (5.7)
Age, y	60 (51–73.5)	51 (48–57)	56 (50–70)	62 (55–68.5)
Women	15 (62.5)	3 (33.3)	6 (35.3)	2 (66.7)
BMI, kg/m^2	28.3 (25.8–31)	29.5 (28.6–32)	30.7 (26.8–33.7)	29.1 (29–34.5)
Symptom onset, d	7.5 (6–10)	7 (5.5–9)	8.5 (5–10.7)	7 (7–7)
SAPS III	58.5 (41.7–76)	50 (39–67)	46 (39–62)	84 (79–84.5)
NEWS	13 (11.7–14)	12 (11–13)	11 (10–13)	12 (11–13)
Ventilation time before enrollment, d	1 (1–2)	2 (1–3)	1 (1–3)	1 (1–1.5)
Use of NIV before intubation	12 (50)	3 (33.3)	8 (47.1)	0 (0)
Driving airway pressure, cm H$_2$O	13 (10.7–14.5)	13 (10–14)	13 (9–15)	9 (8.5–12.5)
Comorbidity				
Systemic arterial hypertension	13 (54.2)	4 (44.4)	8 (47.1)	2 (66.7)
Diabetes	8 (33.3)	1 (11.1)	3 (17.6)	1 (33.3)
Chronic kidney failure	2 (8.3)	0 (0)	2 (11.8)	1 (33.3)

Data are shown as median (25th to 75th percentiles) or *n* (%).
BMI = body mass index
SAPS = Simplified Acute Physiology Score
NEWS = national early warning score
NIV = noninvasive ventilation

dorsal ventilation (pattern 1), 9 subjects (17%) showed bilateral dorsal hypoventilation (pattern 2), 17 subjects (32%) showed unilateral dorsal hypoventilation (pattern 3), and 3 subjects (5.7%) showed unilateral hypoventilation (pattern 4). C_{RS} was comparable among the distribution pattern of hypoventilated regions (Fig. 1B). P_{aO_2}/F_{IO_2} was lower in pattern 2 compared with pattern 1 (Fig. 1C).

Discussion

To our knowledge, this is the first study to demonstrate the utility of EIT in detecting the heterogeneous topographic distribution of lung disease in the subjects with COVID-19–related ARDS. Analysis of our data indicates a higher prevalence of subjects with preserved bilateral dorsal ventilation, followed by unilateral and bilateral dorsal hypoventilation. Analysis of these results suggests a heterogeneous EIT-topographic distribution of the lung disease in ARDS, as reported by previous CT studies.[4-6]

We defined the EIT patterns (or phenotypes) based on a previous CT study,[7] which dichotomized the phenotype of ARDS as a non-focal (corresponding to EIT pattern 1) or focal disease (corresponding to EIT patterns 2, 3, and 4). EIT patterns 3 and 4 were idealized to allow the classification of unilateral lung involvement. We did not include in the current classification the hypoventilation alone in the anterior quadrants due to the risk of interference by the heart area and pulmonary hyperinflation, reducing the ventilation in non-gravity–dependent regions. The threshold of ventilation distribution was defined based on the known range of error between EIT and CT for anterior versus posterior and right versus left regions (bias of 0%

and limits of agreement of 10%).[12] Thus, for instance, the EIT image that shows dorsal ventilation < 40% has a high accuracy to suggest the existence of a regional lung impairment (eg, atelectasis, consolidation).

This report intends to show how EIT can add information to identifying topographic disease distribution in ARDS. For instance, analysis of our data suggests that the subjects with preserved bilateral dorsal ventilation (pattern 1) had comparable C_{RS} with those with bilateral dorsal hypoventilation (pattern 2, which is usually related to regional dorsal consolidations or atelectasis). Therefore, the identification of a patient with pattern 1 can exclude any hypothesis about focal disease presentation. At the same time, the combined information about EIT pattern 1 with high or low C_{RS} can address the severity and/or progression of a non-focal ARDS (eg, patients with minimal or severe diffuse ground-glass opacities).[9] Furthermore, the global C_{RS} was not an informative variable to detect the extension of hypoventilated areas (eg, pattern 2 vs pattern 3 and pattern 2 vs pattern 4), and P_{aO_2}/F_{IO_2} tended to be lower in the subjects with bilateral dorsal hypoventilation, possibly due to the increased shunt area.

We believe that EIT bedside information supports a step forward in clinical studies, in testing ventilatory strategies tailored to lung imaging. For instance, body positioning, such as prone positioning, has frequently been used in patients with ARDS to improve oxygenation by promoting dorsal lung recruitment.[13,14] We found that only one-sixth of our subjects had bilateral dorsal hypoventilation. On the other hand, the greater prevalence of unilateral dorsal hypoventilation may indicate the use of lateral positioning, with the sick lung region positioned up to favor alveolar recruitment.[15] The

small sample size from a single center limited a strong conclusion from our data. Thus, future studies are needed to investigate the role of EIT phenotypes on clinical outcomes. In conclusion, the present study demonstrates a heterogeneous EIT topographic distribution of lung disease in subjects with COVID-19–related ARDS. In addition, standard global parameters such as C_{RS} and P_{aO_2}/F_{IO_2} were almost indistinguishable among the EIT phenotypes.

REFERENCES

1. Ashbaugh DG, Bigelow DB, Petty TL, Levine BE. Acute respiratory distress in adults. Lancet 1967;2(7511):319-323.

2. ARDS Definition Task Force; Ranieri VM, Rubenfeld GD, Thompson BT, Ferguson ND, Caldwell E, et al. Acute respiratory distress syndrome: the Berlin Definition. JAMA 2012;307(23):2526-2533.

3. Maunder RJ, Shuman WP, McHugh JW, Marglin SI, Butler J. Preservation of normal lung regions in the adult respiratory distress syndrome. Analysis by computed tomography. JAMA 1986;255(18):2463-2465.

4. Gattinoni W, Pesenti A, Avalli L, Rossi F, Bombino M. Pressure-volume curve of total respiratory system in acute respiratory failure computed tomographic scan study. Am Rev Respir Dis 1987;136 (3):730-736.

5. Salehi S, Abedi A, Balakrishnan S, Gholamrezanezhad A. Coronavirus disease 2019 (COVID-19): a systematic review of imaging findings in 919 patients. AJR Am J Roentgenol 2020;215(1):87-93.

6. Yu M, Xu D, Lan L, Tu M, Liao R, Cai S, et al. Thin-section chest CT imaging of COVID-19 pneumonia: a comparison between patients with mild and severe disease. Radiol Cardiothorac Imaging 2020;2(2): e200126.

7. Constantin J-M, Jabaudon M, Lefrant J-Y, Jaber S, Quenot J-P, Langeron O, et al; AZUREA Network. Personalized mechanical ventilation tailored to lung morphology versus low positive end-expiratory pressure for patients with acute respiratory distress syndrome in France (the LIVE study): a multicenter, single-blind, randomized controlled trial. Lancet Respir Med 2019;7(10):870-880.

8. Bachmann MC, Morais C, Bugedo G, Bruhn A, Morales A, Borges JB, et al. Electrical impedance tomography in acute respiratory distress syndrome. Crit Care 2018;22(1):263.

9. Morais CCA, Safaee Fakhr B, De Santis Santiago RR, Di Fenza R, Marutani E, Gianni S, et al. Bedside electrical impedance tomography unveils respiratory "chimera" in COVID-19. Am J Respir Crit Care Med 2021;203(1):120-121.

10. Gallagher JT, Ives KL, Cheifetz IM. Electrical impedance tomography in mechanically ventilated children: will it impact clinical care? Respir Care 2022;67(4):494-495.

11. Villar J, Fernández RL, Ambrós A, Parra L, Blanco J, Domínguez-Berrot AM, et al; Acute Lung Injury Epidemiology and Natural history Network. A clinical classification of the acute respiratory distress syndrome for predicting outcome and guiding medical therapy*. Crit Care Med 2015;43(2):346-353.

12. Victorino JA, Borges JB, Okamoto VN, Matos GFJ, Tucci MR, Caramez MPR, et al. Imbalances in regional lung ventilation: a validation study on electrical impedance tomography. Am J Respir Crit Care Med 2004;169(7):791-800.

13. Kallet RH. A comprehensive review of prone position in ARDS. Respir Care 2015;60(11):1660-1687.

14. La Vita CJ, De Santis Santiago RR. Prone position: a strategy in expansion? Respir Care 2021;66(5):884-885.

15. Roldán R, Rodriguez S, Barriga F, Tucci M, Victor M, Alcala G, et al. Sequential lateral positioning as a new lung recruitment maneuver: an exploratory study in early mechanically ventilated Covid-19 ARDS patients. Ann Intensive Care 2022;12(1):13.